

REPORT DOCUMENTATION PAGE

*Form Approved
OMB No. 0704-0188*

Public reporting burden for this collection of information is estimated to average 1 hour per response, including the time for reviewing instructions, searching existing data sources, gathering and maintaining the data needed, and completing and reviewing this collection of information. Send comments regarding this burden estimate or any other aspect of this collection of information, including suggestions for reducing this burden to Department of Defense, Washington Headquarters Services, Directorate for Information Operations and Reports (0704-0188), 1215 Jefferson Davis Highway, Suite 1204, Arlington, VA 22202-4302. Respondents should be aware that notwithstanding any other provision of law, no person shall be subject to any penalty for failing to comply with a collection of information if it does not display a currently valid OMB control number. PLEASE DO NOT RETURN YOUR FORM TO THE ABOVE ADDRESS.

1. REPORT DATE (DD-MM-YYYY) 08-09-2006	2. REPORT TYPE Journal Article	3. DATES COVERED (From - To)		
4. TITLE AND SUBTITLE Measurements and Computations of Mass Flow and Momentum Flux through Short Tubes in Rarefied Gases (POSTPRINT)			5a. CONTRACT NUMBER	
			5b. GRANT NUMBER	
			5c. PROGRAM ELEMENT NUMBER	
6. AUTHOR(S) T.C. Lilly and S.F. Gimelshein (USC); A.D. Ketsdever (AFRL/PRSA); and G.N. Markelov (The Netherlands)			5d. PROJECT NUMBER 50260568	
			5e. TASK NUMBER	
			5f. WORK UNIT NUMBER	
7. PERFORMING ORGANIZATION NAME(S) AND ADDRESS(ES) Air Force Research Laboratory (AFMC) AFRL/PRSA 10 E. Saturn Blvd. Edwards AFB CA 93524-7680			8. PERFORMING ORGANIZATION REPORT NUMBER AFRL-PR-ED-JA-2005-293	
9. SPONSORING / MONITORING AGENCY NAME(S) AND ADDRESS(ES) Air Force Research Laboratory (AFMC) AFRL/PRS 5 Pollux Drive Edwards AFB CA 93524-7048			10. SPONSOR/MONITOR'S ACRONYM(S)	
			11. SPONSOR/MONITOR'S NUMBER(S) AFRL-PR-ED-JA-2005-293	
12. DISTRIBUTION / AVAILABILITY STATEMENT Approved for public release; distribution unlimited. AFRL-ERS-PAS-2005-200.				
13. SUPPLEMENTARY NOTES ©2006 American Institute of Physics, published in Physics of Fluids 18, 093601 (2006)				
14. ABSTRACT Gas flows through orifices and short tubes have been extensively studied from the 1960s through the 1980s for both fundamental and practical reasons. These flows are a basic and often important element of various modern gas driven instruments. Recent advances in micro- and nanoscale technologies have paved the way for a new generation of miniaturized devices in various application areas, from clinical analyses to biochemical detection to aerospace propulsion. The latter is the main area of interest of this study, where rarefied gas flow into a vacuum through short tubes with thickness-to-diameter ratios varying from 0.015 to 1.2 is investigated both experimentally and numerically with kinetic and continuum approaches. Helium and nitrogen gases are used in the range of Reynolds numbers from 0.02 to 770 (based on the tube diameter), corresponding to Knudsen numbers from 40 down to about 0.001. Propulsion properties of relatively thin and thick tubes are examined. Good agreement between experimental and numerical results is observed for mass flow rate and momentum flux, the latter being corrected for the experimental facility background pressure. For thick-to-thin tube ratios of mass flow and momentum flux versus pressure, a minimum is observed at a Knudsen number of about 0.5. A short tube propulsion efficiency is shown to be much higher than that of a thin orifice. The effect of surface specularity on a thicker tube specific impulse was found to be relatively small. ©2006 American Institute of Physics. (DOI:10.1063/1.2345681)				
15. SUBJECT TERMS				
16. SECURITY CLASSIFICATION OF: a. REPORT Unclassified		17. LIMITATION OF ABSTRACT A	18. NUMBER OF PAGES 12	19a. NAME OF RESPONSIBLE PERSON Dr. Ingrid J. Wysong 19b. TELEPHONE NUMBER (include area code) N/A
Standard Form 298 (Rev. 8-98) Prescribed by ANSI Std. Z39.18				

Measurements and computations of mass flow and momentum flux through short tubes in rarefied gases

T. C. Lilly and S. F. Gimelshein

University of Southern California, Los Angeles, California 90089

A. D. Ketsdever

Air Force Research Laboratory, Propulsion Directorate, Edwards Air Force Base, California 93524

G. N. Markelov

Advanced Operations and Engineering Services, 2332 KG Leiden, The Netherlands

(Received 6 February 2006; accepted 31 July 2006; published online 8 September 2006)

Gas flows through orifices and short tubes have been extensively studied from the 1960s through the 1980s for both fundamental and practical reasons. These flows are a basic and often important element of various modern gas driven instruments. Recent advances in micro- and nanoscale technologies have paved the way for a generation of miniaturized devices in various application areas, from clinical analyses to biochemical detection to aerospace propulsion. The latter is the main area of interest of this study, where rarefied gas flow into a vacuum through short tubes with thickness-to-diameter ratios varying from 0.015 to 1.2 is investigated both experimentally and numerically with kinetic and continuum approaches. Helium and nitrogen gases are used in the range of Reynolds numbers from 0.02 to 770 (based on the tube diameter), corresponding to Knudsen numbers from 40 down to about 0.001. Propulsion properties of relatively thin and thick tubes are examined. Good agreement between experimental and numerical results is observed for mass flow rate and momentum flux, the latter being corrected for the experimental facility background pressure. For thick-to-thin tube ratios of mass flow and momentum flux versus pressure, a minimum is observed at a Knudsen number of about 0.5. A short tube propulsion efficiency is shown to be much higher than that of a thin orifice. The effect of surface specularity on a thicker tube specific impulse was found to be relatively small. © 2006 American Institute of Physics.

[DOI: [10.1063/1.2345681](https://doi.org/10.1063/1.2345681)]

I. INTRODUCTION

Low thrust propulsion systems have attracted significant attention over the last few years due to their potential application in future micro- and nanosatellites. Various orbital maneuvers, such as fine pointing and orbital maintenance, will require micropulsion systems with thrust levels in the range from 1 N to as low as 1 mN to counter the effects of orbital perturbations. The low thrust levels imply either low pressure operation or a decrease in the throat dimensions, both leading to low Reynolds number flows. The further development of efficient microchemical and electrothermal thrusters is associated with higher combustion chamber temperatures and will therefore also continue the trend toward a decreasing Reynolds number for nozzle flows. Therefore, the investigation of low Reynolds number nozzle flows, both experimental and numerical, has become increasingly important for designing efficient low thrust nozzles.

It is well known that the Reynolds number is a measure of the nozzle efficiency in terms of the viscous losses inherent in the subsonic layer near the nozzle surfaces. For a given stagnation pressure and temperature, the thrust decreases with the square of the characteristic diameter of the nozzle throat, while the Reynolds number only decreases linearly. Therefore, the geometric scaling of nozzles, i.e., decrease in the throat dimensions, for low thrust appears favorable. The availability of microfabrication techniques allows for nozzle

throats on the order of several micrometers creating the possibility of efficient low thrust systems primarily through the scaling of the throat diameter. In practice, however, systems limitations of microsatellites may force micronozzle propulsion systems to operate at low Reynolds numbers due to small nozzle dimensions as well as lower chamber pressures.¹ From an overall microsatellite systems point of view, storing propellant on-orbit as a liquid or solid has obvious benefits in terms of available storage volume and tankage mass. Because available power on microsatellites is also quite limited, low pressure operation will most likely result from liquid vaporization or solid sublimation propulsion concepts.

At sufficiently low Reynolds numbers, the viscous losses within a micronozzle become large enough for the specific impulse along the nozzle centerline to decrease from the nozzle throat to the exit plane making the concept of a nozzle expansion useless. In the transitional flow regime, therefore, a thin-walled sonic orifice or a short circular tube may perform as well as a typical micronozzle.²

Gas flows through circular orifices and short and long tubes have been rigorously studied in the past, and extensive summaries may be found in Refs. 3 and 4 and references therein. Therefore, here we mention only few of them. Free molecular and transitional flow in tubes and ducts was first studied experimentally and theoretically by Knudsen,⁵ who

examined the dependence of the conductance at different pressure and geometrical parameters. He observed a conductance minimum at $\text{Kn} \approx 1$ for long ducts and tubes. A qualitative explanation for conductance minimum was suggested in Ref. 6. The minimum was attributed to a small population of molecules that enter the tube or reflect on the tube surface with a very small radial velocity. These molecules give a disproportionately large contribution to the mass flow at high Knudsen numbers. As the Knudsen number decreases, molecular collisions disrupt the path of such molecules, therefore decreasing the mass flow. A further increase in the molecular collision frequency stimulates an overall drift velocity that in turn increases the mass flow through the tube.

The conductance and the transmission probabilities in long tubes and channels in the transitional flow has been extensively studied in the 1960s and 1970s, both experimentally⁷ and analytically.⁸ There were also several studies aimed at flows through short tubes and apertures.^{9,10} An example of such studies is in Ref. 11, where the effect of round edges on mass flow was analyzed. This type of flow was also investigated in detail in the past decade, most noticeably with respect to emerging micro- and nanotechnologies (such as lubrication problems that deal with transitional flows in long channels and tubes) and porous media (represented by a single or multiple capillaries). Many researchers have made a significant contribution to the field, such as Ref. 12, where a method for solving low-velocity microflows by scaling the temperature of the fluid such that the molecular thermal velocity is on the same order of magnitude as the fluid velocity; Ref. 13, where the mass flow, heat flux, and diffusion flux of rarefied gas mixture through long tubes caused by gradients of pressure, temperature, and concentration were calculated; and Ref. 14, where rarefied gas flows in thin film slider bearings are studied in a wide range of Knudsen numbers.

Although an extensive knowledge has been accumulated on transitional flows in orifices and short tubes, there have been few investigations of these geometries from the point of view of micropulsion, which requires a detailed study of the mass flow rate, momentum flux, and specific impulse.^{15–17} The importance of such a study is related to the lack of information on a specific impulse for the above geometries, that was emphasized in Refs. 18 and 19, where gas flow in a Free Molecule Micro-Resistojet was examined experimentally.

The primary scope of this work is experimental and numerical study of this effect in short circular tubes as compared to a thin-walled orifice. In this study we also extend the low end of the Reynolds number range that previous studies have investigated by extending operating conditions down to the free molecule flow regime. To the best of the author's knowledge, this represents the first work, where momentum flux through short tubes in rarefied flow has been measured.

The experiments and computations were conducted at room temperature, using nitrogen and helium with stagnation pressures from 1 to 5000 Pa. The computations are performed using two different approaches: a kinetic approach (the direct simulation Monte Carlo method, DSMC) and a

continuum approach (a solution of the Navier-Stokes equations, NS hereafter).

II. EXPERIMENTAL SETUP AND FLOW CONDITIONS

All measurements were performed on the nano-Newton Thrust Stand (nNTS), which has been described in detail in Ref. 1 and specially modified for this experiment's particular needs. The nNTS was installed in Chamber IV of the Collaborative High Altitude Flow Facilities (CHAFF-IV), which is a 3 m diameter by 6 m long cylindrical, high vacuum chamber. The facility was pumped with a 1 m diameter diffusion pump with a pumping speed of 42 000 L/s for helium and 25 000 L/s for molecular nitrogen in conjunction with a turbomolecular pump with a pumping speed of 3500 L/s for molecular nitrogen. The ultimate facility pressure was approximately 10^{-4} Pa with all operational pressures below 0.1 Pa. Measurements of the chamber background pressure were taken with an absolute pressure transducer in conjunction with an ionization gauge.

The thickness of the tube, t , was varied from 0.015 mm to 1.2 mm, while the diameter d was constant at 1 mm. All considered geometries were sharp edged. The tube was attached to a plenum with a cross-sectional area much larger than the tube area to help ensure uniform flow. The thinnest tube was machined in a 0.015 mm thick tantalum shim giving $t/d=0.015$. The medium and thickest tubes were machined into aluminum plates with t/d values of 0.508 and 1.2, respectively. The plenum size ($66 \times 35 \times 17.5$ mm) is the same for all three geometries.

The stagnation pressures were measured through taps on the side of the plenums using calibrated differential pressure transducers. The carrier gas was introduced to the plenum through an adjustable needle valve located downstream of a mass flow meter. In the experimental configuration, the mass flow meters were operated in the continuum regime throughout the pressure range investigated. The gases used were molecular nitrogen and helium. The stagnation pressures ranged from 1 Pa to 5000 Pa. The stagnation temperature was measured to be 295 K in equilibrium with ambient. The combination of stagnation pressure and temperature gave a maximum Reynolds number of 770 for nitrogen and about 290 for helium, based on the tube diameter.

The nNTS was calibrated using electrostatic calibration techniques described by Selden.¹⁹ A unique feature of the nNTS is its ability to measure the force levels of a 1.0 mm tube from the free molecule through continuum range. The low force measuring capability of the nNTS allowed for the investigation of the transitional flow regime overlooked in previous low Reynolds number studies.

III. NUMERICAL APPROACHES

Two approaches, kinetic and continuum, are used in this study to model gas expansion into vacuum. The kinetic approach (DSMC method) is used for the entire range of pressures under consideration. The continuum method (solution of Navier-Stokes equations) is applied for pressures 35 Pa and higher, where the flow regime changes from transitional to near continuum.

A. Kinetic approach

The DSMC-based software system SMILE²⁰ was used in all DSMC computations. The majorant frequency scheme²¹ was used to calculate intermolecular interactions. The intermolecular potential was assumed to be a variable hard sphere.²² Energy redistribution between the rotational and translational modes was performed in accordance with the Larsen-Borgnakke model. A temperature-dependent rotational relaxation number was used. The reflection of molecules on the surface was assumed to be diffuse with complete energy accommodation.

The DSMC method is conventionally used to model supersonic and hypersonic flows, where the boundary conditions are either supersonic inflow or vacuum outflow. Their implementation for these cases is straightforward. For subsonic flows, such as the flow inside the stagnation chamber, the application of the DSMC method is more complicated. In the present study, a large computational domain was used so that the disturbances arising downstream do not significantly influence the flow near the subsonic boundaries. This allows one to use constant flow properties at these boundaries. Zero flow velocity was assumed at the inflow boundaries, with the pressure and temperature corresponding to given stagnation conditions.

The impact of the computational domain was found to have no visible effect on flow parameters, both distributed and integral, when the domains of 8×4 mm and 16×8 mm were examined. The smaller one was therefore used in all computations presented below. The DSMC modeling was performed for two different sets of numerical parameters, about 25 million molecules and 10 million cells for pressure larger than 2000 Pa, and about 3 million molecules and 1 million cells for pressures smaller than 2000 Pa. These numbers were used to satisfy the DSMC requirements for the linear cell size be less than the gas mean free path, λ (the cell size was about the mean free path for the most dense case of 5200 Pa in nitrogen), and the number of molecules in a λ^2 area be larger than one (at least two were taken). The time of 0.2 ms was found to be sufficient to reach steady state. The macroparameter sampling was performed over 100 000 time steps of 3 ns for the first set, and 100 000 time steps of 80 ns for the second set, with a typical statistical error in flow fields below 2%, and in mass flow and momentum flux below 0.4%.

B. Continuum approach

The Navier-Stokes computations were performed with commercial software, CFD-ACE, which is a pressure-based finite-volume flow solver (CFD-Ace: User Manual, Version 2003, CFD Research Corporation, 2003). CFD-ACE is a set of computer programs for multiphysics computational analysis. It is designed to simulate steady and unsteady flows, perfect gas and multispecies reacting flows.

The following features of CFD-ACE are used for present computations: structured grid solver, conjugate gradient squared method with preconditioning, algebraic multigrid solver, Sutherland law for the viscosity, and slip boundary conditions on plenum and tube walls. These conditions al-

lowed us to obtain reliable, stable, and converged solutions for significantly lower stagnation pressures than in Ref. 17 (410 against 3570 Pa). Boundary conditions with a fixed value of stagnation pressure at the inflow boundaries and a fixed value of pressure at the outflow boundaries are applied. The prescribed value of the outflow pressure is four orders of magnitude lower than the stagnation pressure, and used primarily for the transient stage of computations. If the Mach number at the outflow boundary exceeds unity, the solver automatically switches the conditions to extrapolation from internal nodes. The computational domain is 7×4 mm, and a multiblock grid is used consisting of 71 000 to 88 000 nodes depending on the tube thickness. The nodes are clustered to the tube in order to properly resolve strong flow gradients in this region. Note that an increase of the computational domain or a decrease in the number of nodes did not have visible effect on the mass flow rate and momentum flux. For example, doubling the number of nodes in the vicinity and inside of the tube (the total number of nodes was changed from 51 000 to 71 000) for helium at a stagnation pressure of 5200 Pa changes mass flow rate and momentum flux only by 0.2% and 0.1%, respectively.

IV. EXPERIMENTAL AND NUMERICAL UNCERTAINTIES

There are several possible sources of experimental uncertainties in this work. First, there is always a finite background gas pressure in the chamber that increases with mass flow. The background gas may impact the mass flow measurements only for stagnation pressures larger than 1500 Pa, although the force (momentum flux) measurements are affected to some extent at all plenum pressures. A previous study²³ indicated that the force can be affected by less than 0.5% at the experimental conditions of this work. The previous study is supplemented here with the numerical modeling in order to quantify the facility effect on force measurements. Another source is the standard deviation of the stagnation pressure and mass flow measurements; those were found to be within approximately 1% over the range used. For the momentum flux measurements, a stand calibration of deflection angle versus applied force has been approximated to be within 3%. For a given applied force to the stand, the standard deviation of the stand's deflection was less than 1%; however, the accuracy of the calibration system must also be taken into account. Finally, there was some error associated with the manufacturing of the tubes. In general, the tube diameter of thicker tubes, manufactured of aluminum, is known to be within 0.2%. The thinnest configuration was machined from a thin tantalum shim, and the measurement of its diameter is therefore not quite as accurate and is estimated to be within approximately 2%.

In addition to the experimental uncertainties, there are a number of numerical uncertainties. Grid resolution, the maximum number of simulated molecules, effects of the subsonic boundary conditions, and the gas-gas collision models were all found to be within the statistical error of the DSMC computations mentioned above, and may account for a numerical uncertainty estimated to be on the order of 1% to

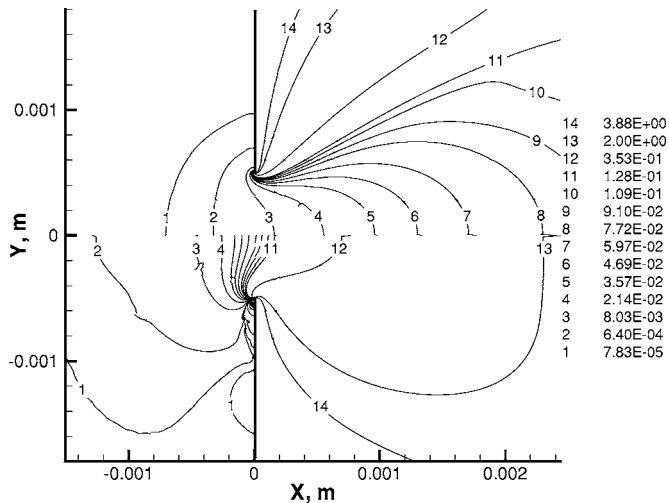


FIG. 1. Local Knudsen number for $t/d=0.015$. Helium flow, $P_0=5200$ Pa (top) and $P_0=410$ Pa (bottom).

2%. The effects of the tube surface roughness present in the experimental device are not known, and a simple diffuse scattering model was used.

V. FLOW SOLUTIONS BY KINETIC AND CONTINUUM APPROACHES

The two approaches, kinetic and continuum, are used to model gas flows through short tubes for the higher pressures under consideration, which allows us to address the accuracy issues of the numerical solutions. It is well known that the Boltzmann equation, and therefore the DSMC method, is applicable to simulate gas flows in the binary collision regime. This regime is observed at pressures up to several atmospheres, which is well above the range of pressures examined in this work. The use of the DSMC method for modeling very low Knudsen number flows, on the order of 0.001 and lower, however, is still raising questions to the numerical accuracy of obtained solutions, primarily related to the number of simulated molecules and cells. This is further magnified by uncertainty in the subsonic boundary conditions, as well as the long time required to reach steady state. The solution of the NS equations, on the other hand, is limited by its area of applicability.

The NS equations may be derived from the Boltzmann equation with the assumption of a small deviation of the velocity distribution function from Maxwellian,

$$f = f_M[1 + O(\text{Kn})].$$

Here, Kn is the local Knudsen number equal to the ratio of the local mean free path to a distance $\rho/(d\rho/dx)$, where ρ is the gas density. The local Knudsen number, Kn , is therefore used to analyze the difference between the continuum and kinetic methods, and therefore the applicability of the continuum results.

The local Knudsen number calculated by the continuum approach for $t/d=0.015$ in helium is plotted in Fig. 1. Gas expansion through a short tube into vacuum is characterized by strong rarefaction in the region near the outer lip, and one can expect large values of the local Knudsen number with

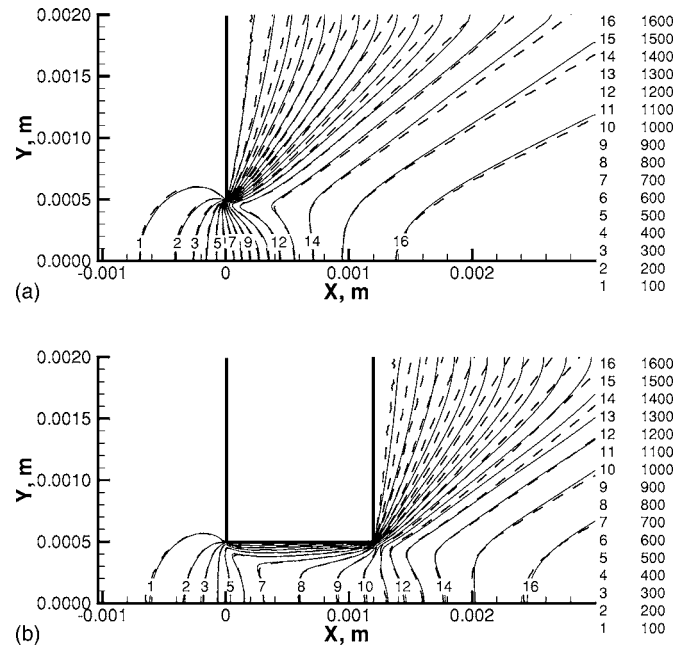


FIG. 2. Helium axial velocity (m/s) at $P_0=5200$ Pa obtained by kinetic (dashed lines) and continuum (solid lines) approaches, $t/d=0.015$ (top) and $t/d=1.2$ (bottom).

the continuum approach failing in that region. For the highest plenum pressure under consideration of 5200 Pa, the value of the local Knudsen number at the exit plane reaches 0.1 near the surface. At as much as quarter of the exit area, it is larger than the value of 0.2 found to correlate with the breakdown of the continuum approach. The values of the local Knudsen number increase by over an order of magnitude as the pressure decreases to 410 Pa, which corresponds to the diameter-based Knudsen number of 0.0425. In this case, the 0.2 isoline lies in the subsonic region inside the plenum, and the values at the exit plane change from 0.08 to 0.5 closer to the surface.

A comparison of the macroparameters obtained with the kinetic and continuum approaches shows that the agreement is very good between the two for higher pressures. This is illustrated in Fig. 2, where the velocity in the axial direction is shown for a helium flow through tubes of different thickness. A comparison of the velocity and the local Knudsen number fields shows that the NS solution is close to the DSMC result in the region, where the local Knudsen number is less than 0.1. The axial velocities are different for the two approaches only in the expansion region where flow angle

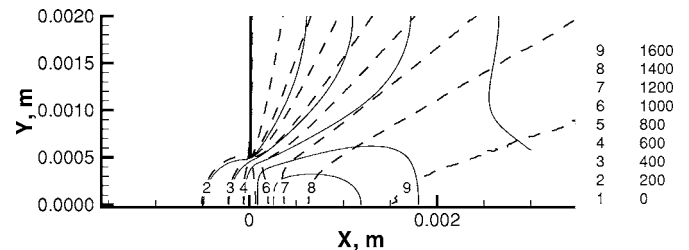


FIG. 3. Helium axial velocity (m/s) at $P_0=410$ Pa obtained by kinetic (dashed lines) and continuum (solid lines) approaches, $t/d=0.015$.

TABLE I. Helium mass flow (kg/s) and momentum flux (N) for different plenum pressures (Pa) and two thickness-to-diameter ratios.

P_0	Kn	$t/d=0.015$				$t/d=1.2$			
		\dot{m} , DSMC $\times 10^{-6}$	\dot{m} , NS $\times 10^{-6}$	F, DSMC $\times 10^{-3}$	F, NS $\times 10^{-3}$	\dot{m} , DSMC $\times 10^{-6}$	\dot{m} , NS $\times 10^{-6}$	F, DSMC $\times 10^{-3}$	F, NS $\times 10^{-3}$
410	0.0425	0.234	0.197	0.302	0.312	0.126	0.164		
1071	0.0163	0.638	0.602	0.877	0.885	0.411	0.376	0.565	0.547
1605	0.0109	0.950	0.927	1.336	1.351	0.662	0.634	0.927	0.912
2142	0.0081	1.252	1.254	1.792	1.819	0.930	0.927	1.305	1.351
3570	0.0049	2.145	2.119	3.040	3.065	1.674	1.670	2.368	2.387
5200	0.0033	3.140	3.105	4.440	4.485	2.576	2.581	3.658	3.686

relative to the plume axis is larger than 30. The difference is primarily attributed to the nonequilibrium between translational modes, with the actual ratio of temperature in the axial direction to the total translational temperature being as small as 0.4. Note also that the account for the velocity slip in the NS solver allows one to match the DSMC solution inside the tube for $t/d=1.2$, whereas the no-slip NS flow fields differ from the DSMC ones near the surface, as was pointed out by Ref. 17.

The decrease in stagnation pressure results in a significant deviation of continuum results from the DSMC, as illustrated in Fig. 3. The difference is relatively small in the regions where the local Knudsen number is less than 0.1, and becomes large downstream of the exit. Note that a similar trend was observed for other macroparameters, such as temperature and density, which generally points to the inapplicability of the continuum solver to predict flows through tubes into vacuum at this Knudsen number.

The lower flow velocities at the exit predicted with the continuum approach (see Fig. 3) result in smaller mass flow rates for low pressures. This is illustrated in Table I, where the helium mass flow and momentum flux are summarized for two thickness-to-diameter ratios and several plenum pressures. The results show that the continuum solution significantly deviates from the kinetic one at $Kn>0.01$. This conclusion holds both for $t/d=0.015$ and $t/d=1.2$. For $t/d=1.2$, the difference in the mass flow reaches 5% for $Kn=0.0109$ and 10% for $Kn=0.016$, with the continuum mass flow being lower, even though the velocity slip was included in the calculations. For plenum pressures larger than 2000 Pa, corresponding to $Kn<0.008$, the difference between the two approaches is less than 1%, within the computational error, even for conditions when the local Knudsen

number at the exit is as big as 0.3. For the largest pressure under consideration, the NS computations were also performed with the no-slip boundary conditions. For those computations, the mass flow was about 1.5% and the momentum flux about 0.5% lower than the corresponding values with slip.

Numerical modeling of flows through short tubes has shown that for a diatomic gas the area of validity of the continuum solver in terms of Knudsen number is similar to the monatomic gas flow. This is illustrated in Table II for $t/d=0.015$, where the nitrogen properties are listed. For larger t/d , the agreement between the DSMC and NS solutions at $Kn\approx 0.01$ is better for nitrogen than for helium. At $Kn<0.01$, the difference between the DSMC and NS is within the boundaries of numerical error both for the mass flow and momentum flux.

It is interesting to note that when the plenum pressure is large enough the momentum flux through a $t/d=0.015$ tube is close for helium and nitrogen (compare the continuum values of 4.485×10^{-3} N for helium and 4.486×10^{-3} N for nitrogen at $P_0=5200$ Pa). This is explained as follows. The main differences between nitrogen and helium in terms of modeling momentum flux are mass, gas-surface interaction, and internal energy modes. The latter does not impact the flow inside the plenum or in the vicinity of the exit since the surface temperature is equal to the stagnation temperature. The gas-surface interaction does not play an important role for $t/d=0.015$. The first factor, the mass, should not significantly affect the force measured at the exit (i.e., close to the sonic line), since the momentum flux at the sonic line is essentially a function of the pressure, the area, and the specific heat ratio.

This is shown in Fig. 4, where the DSMC normalized

TABLE II. Nitrogen mass flow (kg/s) and momentum flux (N) for different plenum pressures (Pa) and two thickness-to-diameter ratios.

P_0	Kn	$t/d=0.015$				$t/d=1.2$			
		\dot{m} , DSMC $\times 10^{-6}$	\dot{m} , NS $\times 10^{-6}$	F, DSMC $\times 10^{-3}$	F, NS $\times 10^{-3}$	\dot{m} , DSMC $\times 10^{-6}$	\dot{m} , NS $\times 10^{-6}$	F, DSMC $\times 10^{-3}$	F, NS $\times 10^{-3}$
410	0.0133	0.634	0.601	0.334	0.312	0.419	0.413	0.224	0.231
1071	0.0051	1.658	1.621	0.907	0.918	1.282	1.284	0.706	0.717
3570	0.0015	5.520	5.443	3.093	3.079	4.869	4.912	2.724	2.752
5200	0.0010	8.037	7.924	4.519	4.486	7.275	7.369	4.080	4.129

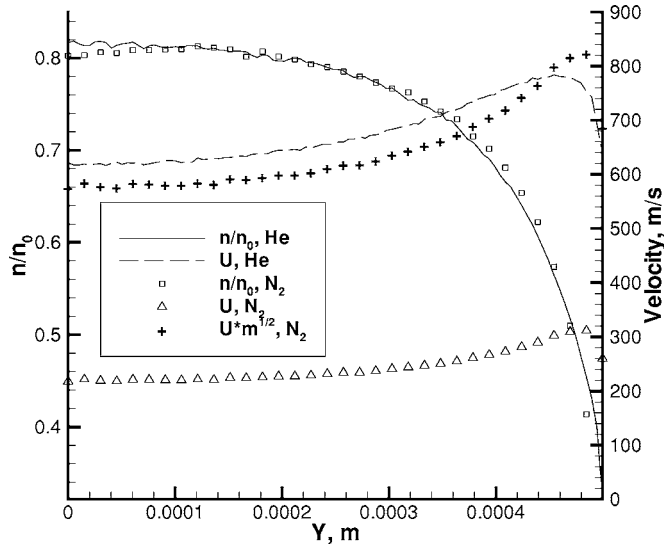


FIG. 4. Normalized density and velocity profiles along the exit for two gases. $t/d=0.15$, $P_0=3570$ Pa. Here, $m=m(\text{N}_2)/m(\text{He})$.

density and velocity profiles are given along the exit for a stagnation pressure of 3570 Pa. The axis is located at $Y=0$. It is seen that there is a negligible difference between the number density profiles for the two gases. The axial velocity profiles are different by approximately a factor equal to the square root of the mass ratio. To illustrate this, a profile is shown of the variable $U_x(\text{N}_2)\sqrt{m(\text{N}_2)/m(\text{He})}$ (compare it to the helium axial velocity profile). All this results in a very small difference between helium and nitrogen momentum flux values.

VI. NUMERICAL AND EXPERIMENTAL DATA

Mass flow through short tubes has been measured and calculated in a wide range of pressure both for helium and nitrogen. The comparison of the computed and measured mass flows is presented below in terms of a discharge coefficient to better illustrate the differences between the obtained results. The discharge coefficient is the ratio of the actual mass flow to the corresponding value for the one-dimensional (1-D) inviscid flow through a sonic orifice,

$$\dot{m} = \rho^* a^* A^*,$$

where ρ^* and a^* are the gas density and velocity at the throat, determined by the plenum conditions through the isentropic relations (see, for example, Ref. 24), and A^* is the throat area.

The computed and measured values of the discharge coefficient $t/d=0.015$ are presented in Fig. 5. The experimental results are given here for plenum pressures below 1000 Pa; the facility (background gas) effects are negligible in this case. The agreement between the kinetic solution and the experiment is very good for the two gases under consideration. The continuum solution consistently underpredicts the data, although the region where the two overlap is, in fact, outside the applicability region of the continuum solver. The discharge coefficient reaches its continuum values of about 0.86 for nitrogen and 0.83 for helium at pressures of about

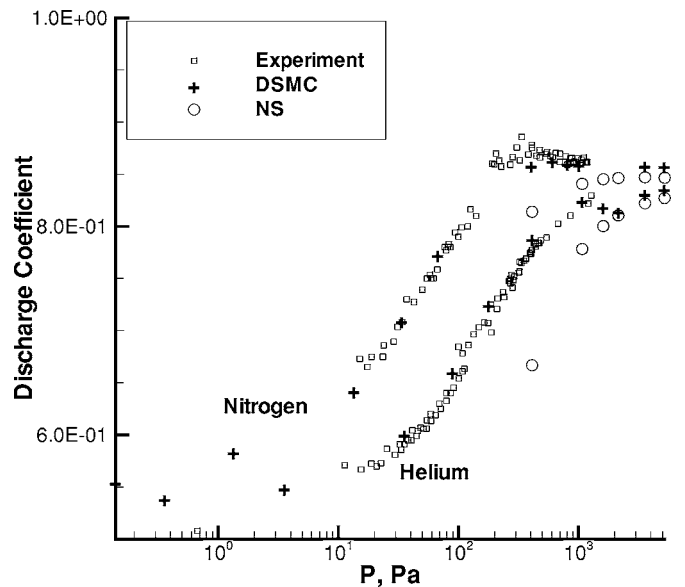


FIG. 5. Discharge coefficient versus plenum pressure for helium and nitrogen at $t/d=0.015$: numerical modeling and experiment.

500 Pa and 2000 Pa, respectively. This corresponds to the Knudsen number of about 0.01. The asymptotic values of 0.86 and 0.83 are in good agreement with previous experimental and numerical studies (see, for example, Refs. 11 and 13).

Note that there is a small maximum in discharge coefficient observed for the nitrogen flow at pressures about 300 Pa. However, the magnitude of this maximum (about or less than 1%) is within both experimental and numerical error, and more accurate data would be necessary to support the existence of the maximum. The kinetic results in the free molecular regime ($\text{Kn}=50$) are somewhat lower than the corresponding theoretical free molecular limits of 0.58 for nitrogen and 0.55 for helium. This is attributed to the finite thickness of the wall of $t/d=0.015$. The number of particles hitting the internal surface of a very short tube amounts to roughly $2t/d$. Since about half of those molecules are returning back to the chamber, the total mass flow is reduced approximately by a factor of $(1-t/d)$.

A comparison of computed and measured discharge coefficients for a larger t/d of 1.2 is presented in Fig. 6. As expected, the formation of the boundary layer inside the tube results in much lower experimental and numerical values of the discharge coefficient in the entire range of pressures under consideration, as compared to $t/d=0.015$. It is also clear that even at pressures above 5000 Pa (Knudsen numbers less than 0.001) the discharge coefficient has not reached continuum limits corresponding to this geometry. Similar to the $t/d=0.015$ case, the discharge coefficient values obtained by the DSMC method are in good agreement with the corresponding experimental values both for helium and nitrogen. For nitrogen, the experimental points are somewhat lower for the high end of pressures, which is attributed to a small but finite effect of the chamber background gas. The continuum solution has a steeper slope than the kinetic and experimental

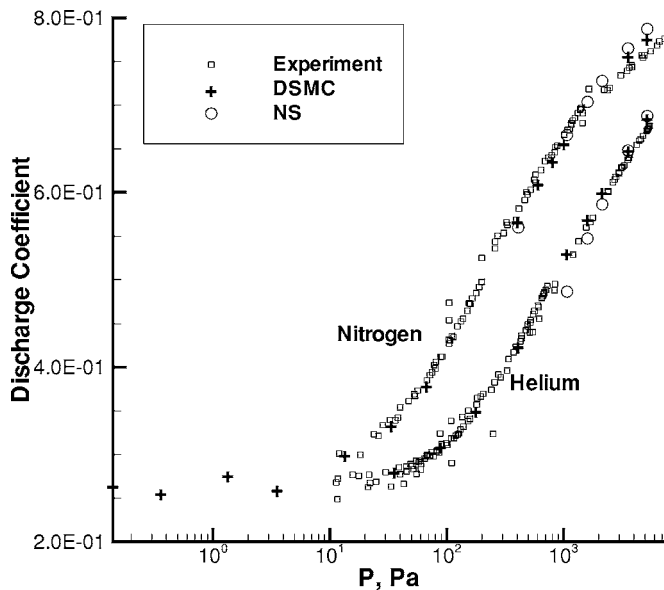


FIG. 6. Discharge coefficient versus plenum pressure for helium and nitrogen at $t/d=1.2$: numerical modeling and experiment.

ones, but is generally in better agreement with the experiment than for $t/d=0.015$.

In this study, the measurements of momentum flux were performed versus mass flow and not pressure. Therefore, it is reasonable to compare the experimental momentum flux with numerical results as a function of mass flow. This allows us to avoid unnecessary uncertainties associated with mass flow versus pressure measurements, and minimize the effect of the experimental tube diameter uncertainty. The comparison of computational and experimental results for $t/d=0.015$ is given in Fig. 7. It is seen that the agreement between the measured and calculated forces is very good, with the exception of the continuum values outside of the applicability lim-

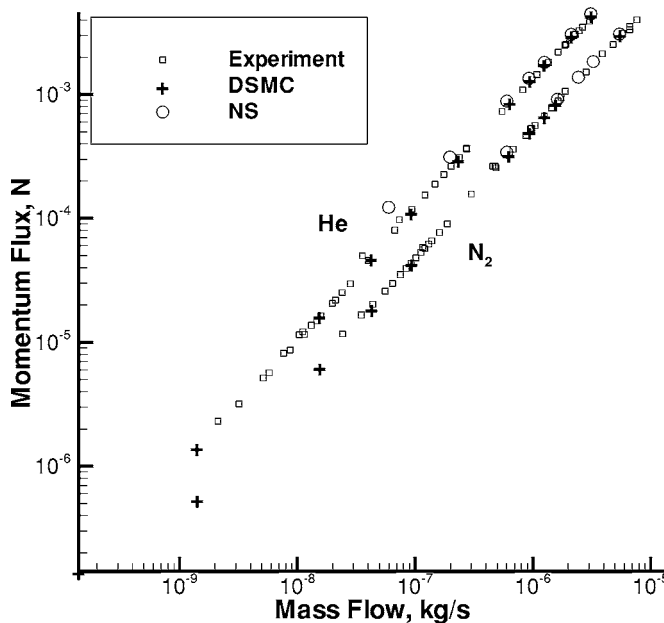


FIG. 7. Momentum flux versus mass flow for helium and nitrogen at $t/d=0.015$: numerical modeling and experiment.

its of the NS approach. The momentum flux changes linearly with the mass flow both for helium and nitrogen. The momentum flux for helium is larger than that for nitrogen by a factor equal to the square root of the inverse ratio of their molecular masses, due to the corresponding difference in the thermal velocities.

One of the important issues in the comparison of measured and computed momentum fluxes is the presence of background molecules in the chamber, which was not accounted for in the above calculations. In the absence of the gas flow through a tube, the background gas in the plenum is uniform, and the momentum flux is the same over all sides of the plenum. When there is a flow through a tube, there are two types of side effects possible that may impact the momentum flux measurements. First, an average velocity of the background gas may be induced in the chamber, different in different locations throughout the chamber. This average velocity may generally either decrease or increase the total force on the plenum. Second, and more important, the plume molecules move background molecules away from the tube (front) side of the plenum,²³ which in turn reduces the background gas pressure on the front side compared to the back side, and acts toward decreasing the total measured momentum flux. This effect is, in fact, even more complex, since there may be also a significant flux of plume molecules coming on the front side. It is clear that this effect is minimum in the continuum flow, and not present in the free molecular flow. However, in the transitional regime the effect is not clear *a priori*, and has to be characterized.

The DSMC computations have therefore been performed to quantify the contribution of the plume-background gas interaction on the total force change. The computations were three dimensional, included the front side of the plenum with the actual dimensions of 0.035×0.066 m and $t=0.015$, and used an inflow starting surface at $M=2$, generated from corresponding the 2-D computations. Helium flow was considered with the stagnation pressures of 410 and 5200 Pa, and the background pressures of 0.01 and 0.11 Pa, respectively. Note that these values of the background pressures were taken from the pressure sensor measurements in the center of the wind side of the chamber. The computations showed that the pressure force on the front side of the plenum is lower than that on the back side, with the difference amounting to about 1% of the corresponding plume force for $P_0=410$ Pa and 0.75% of the plume force for $P_0=5200$ Pa. This difference is considered not significant, and therefore no special correction of the experimental data has been conducted. In order to analyze the impact of the induced background gas flow in the chamber, DSMC computations has also been carried out for $P_0=410$ Pa, that included a full internal geometry of the CHAFF-IV facility with one and two diffusion pumps working. The computations showed that there is no noticeable flow of the background gas in the chamber, and, with the exception of the plume region, it is essentially stagnant at constant temperature and pressure.

The conclusions on negligible facility effects shown numerically for $t=0.015$ are believed to be applicable to the same extent to larger thickness-to-diameter ratios. The increase of t/d generally results in a better flow directionality,

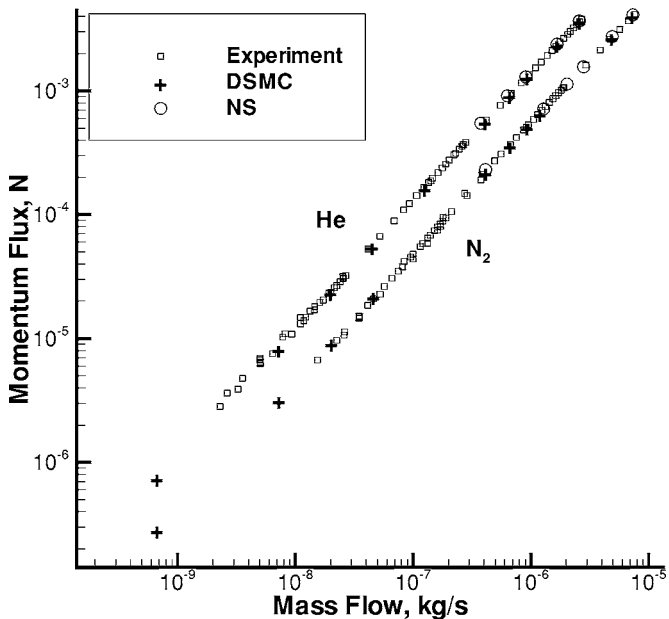


FIG. 8. Momentum flux versus mass flow for helium and nitrogen at $t/d=1.2$: numerical modeling and experiment.

and therefore smaller influence of the plume-background gas interaction on the force on the front side of the plenum. The results of measurements of the momentum flux are given in Fig. 8 for $t/d=1.2$ and two gases. Similar to the $t/d=0.015$ case, the momentum flux is nearly linear versus the mass flow. The numerical predictions of the momentum flux through a tube with $t/d=1.2$, both kinetic and continuum, are in very good agreement with the experimental data in the entire range of considered pressures.

While the facility effects are the primary reason for experimental uncertainties, the most probable reason for numerical inaccuracy is thought to be the uncertainty in the gas-surface interaction model. Obviously, flows with larger t/d are especially sensitive to the choice of this model. Although the agreement between the numerical and experimental data for mass flow and momentum flux speaks for the diffuse model as a reasonable assumption in this case, the DSMC computations have also been performed for $t/d=1.2$ with a Maxwell (specular-diffuse) model with an accommodation coefficient $\alpha_D=0.8$ (20% molecules are reflected specularly, and 80% diffuse). Generally, surface specularity in a straight tube increases the mass flow, and for a fully specular reflection of molecules on the surface the mass flow is the same as for an infinitely thin orifice. For a diffuse-specular reflection, the mass flow is expected to fall between these two limits, with the surface impact being smaller for higher pressures due to a thinner boundary layer. An interesting fact is that surface specularity primarily affects the density field, and not the axial velocity. This is illustrated in Fig. 9, where the normalized density and axial velocity profiles are given along the exit. The results are shown for a plenum pressure of 410 Pa ($\text{Kn}=0.0425$) since the impact of the accommodation coefficient is maximum in this case. Axial velocity for the two α_D parameters almost coincide, except for a small region near the surface where the velocity

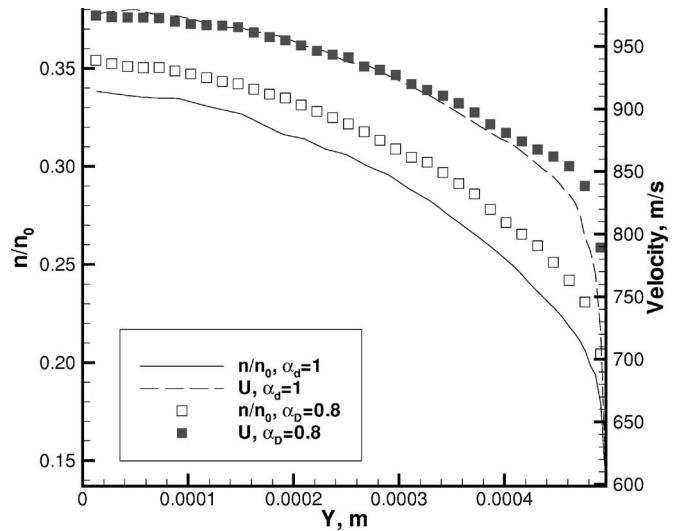


FIG. 9. Normalized density and axial velocity (m/s) profiles at the orifice exit for $\alpha_D=1$ and $\alpha_D=0.8$. Helium, $t/d=1.2$, $P_0=410$ Pa.

of the more specular case is higher. The number density, however, is proportionally lower for $\alpha_D=0.8$ at any location inside the tube exit. The mass flow and the momentum flux for $\alpha_D=0.8$ are $0.136 \times 10^{-6} \text{ kg/s}$ and $0.178 \times 10^{-3} \text{ N}$, respectively. This is an increase about 8% compared to the fully diffuse case. Since the numerical data agree with the measurements within 1 to 2%, the actual surface specularity is much smaller than the assumed 20% for $\alpha_D=0.8$.

VII. INFLUENCE OF WALL THICKNESS ON MASS FLOW AND MOMENTUM FLUX

The friction at the tube surface results in significantly lower mass flows for thicker tubes, even for relatively high pressures. This is illustrated in Fig. 10, where the experimental values of mass flow for different thickness-to-diameter ratios and two gases are presented. Note that the mass flow as a function of pressure is almost linear in the range of pressures from 100 to 2000 Pa, which means that the flow structure essentially does not change for Knudsen numbers $\text{Kn}<0.1$. The situation is different when the tube length becomes comparable to the tube diameter. In this case, the flow slowly transitions from free molecular, when molecules pass through a tube without collisions, to continuum, when the boundary layer thickness becomes negligibly small. This transition is responsible for the noticeable, especially at $t/d=1.2$, curvature of the mass flow versus pressure. This is true both for a monatomic and a diatomic gas. The boundary layer inside the tube significantly lowers that tube throughput, and in the transitional regime the mass flow for $t/d=0.5$ is closer to $t/d=1.2$ than $t/d=0.015$. The momentum flux versus mass flow weakly depends on the tube length (cf. Figs. 7 and 8). The momentum flux for the thickest tube, $t/d=1.2$, is only a few percent higher than that for $t/d=0.015$ for the entire range of considered mass flows.

In order to better understand the reasons for difference between the thinnest and the thickest tubes considered in this work, it is beneficial to examine the thick-to-thin ratios of momentum fluxes and mass flows. These ratios were ob-

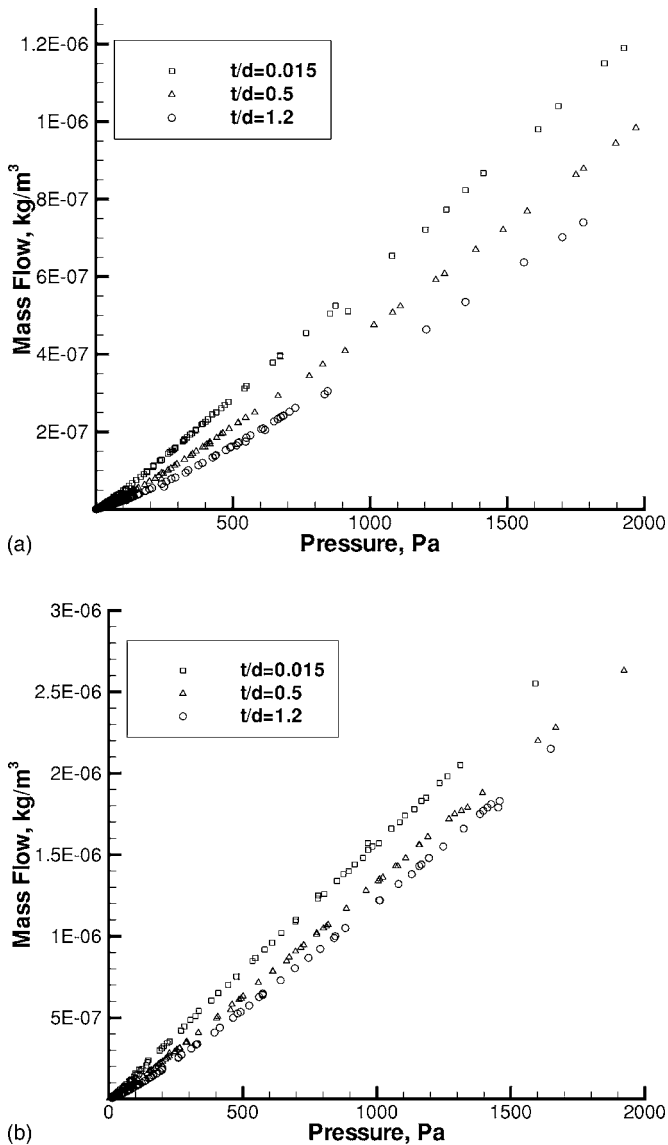


FIG. 10. Measured mass flow as a function of plenum pressure for three t/d ratios. Helium (top) and nitrogen (bottom).

tained at fixed pressures both using the DSMC method and experimentally, and the results are shown in Fig. 11. Both mass flow and momentum flux ratios generally decrease with pressure for pressures ranging from nearly continuum regime down to $P \approx 100$ Pa, which correspond to a Knudsen number of about 0.25. The most remarkable feature is a minimum observed both for mass flow and force ratios at pressures between 50 and 100 Pa ($0.25 < \text{Kn} < 0.5$). After that, the ratios increase slightly toward the free molecular regime.

The minimum is very small, about 1%, for the mass flow ratio, and although it is visible in numerical modeling, it could not be confirmed experimentally due to larger scatter in experimental data. For the momentum flux, however, this minimum amounts to almost 10% of the free molecular value, and is clearly seen both numerically and experimentally, as shown in Fig. 11. The qualitative explanation for the minimum is somewhat similar to that for the Knudsen minimum effect, cited in Sec. I. Let us first compare the flow through tubes with $t/d=0.015$ and $t/d=1.2$ in the free mo-

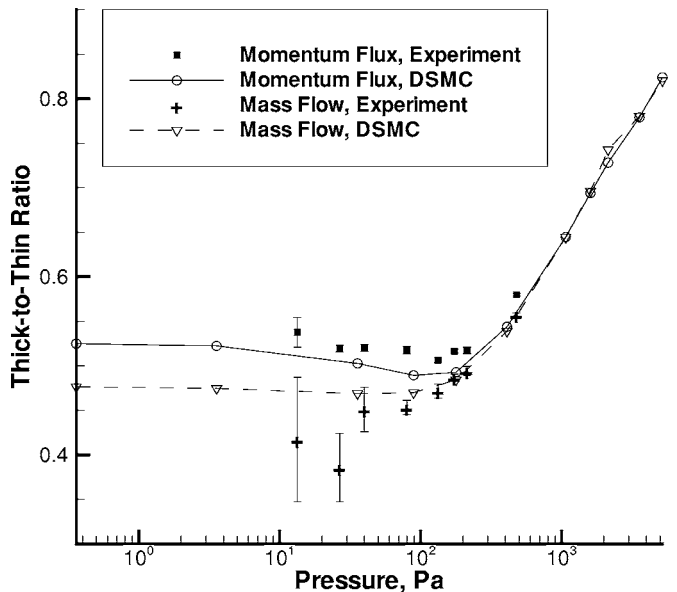


FIG. 11. Ratio of the mass flow and momentum flux for $t/d=1.2$ to the corresponding values at $t/d=0.015$. Helium flow.

lecular regime. Practically all molecules that intersect the tube entrance plane leave the plenum when $t/d=0.015$ (only about 1.5% of the total number of intersecting molecules will return back to the plenum). For a larger thickness, however, the transmission probability may be much lower than unity, depending on t/d ratio, which explains much lower mass flows in this regime.

As the Knudsen number decreases, the effect of collisions for $t/d=1.2$ becomes significant. This effect for relatively high Knudsen numbers results in a decrease in mass flow since molecules that have relatively high axial velocities and whose contribution to mass flow is highest now have a finite probability to collide with molecules that previously collided with the tube surface. The contribution of these high axial velocity molecules therefore goes down as their axial velocity decreases after such collisions. The further decrease in the Knudsen number results in a general drift of molecules downstream toward the exit due to intermolecular collisions. The overall drift velocity increases as the boundary layer inside the tube decreases, thus reducing the difference between mass flow and force obtained for $t/d=1.2$ and $t/d=0.015$.

To examine the observed minimum in more detail, the DSMC computation has been performed for a $t/d=1.2$ tube at $P_0=35.7$ Pa ($\text{Kn}=0.5$), using four chemically identical species characterized as follows: Species 1 is assigned to molecules that come from the upstream boundaries inside the plenum. To see the effect of molecular collisions, species 2 is created from molecules of species 1 after they collide with any other species inside the tube. When molecules of species 1 collide with the tube surface, they are transformed to species 3. Finally, species 4 is created from molecules of species 2 that collide with the tube surface and molecules of species 3 that collide with other molecules inside the tube.

The distribution of mole fractions of these species along the tube axis is shown in Fig. 12. Here, the tube starts at

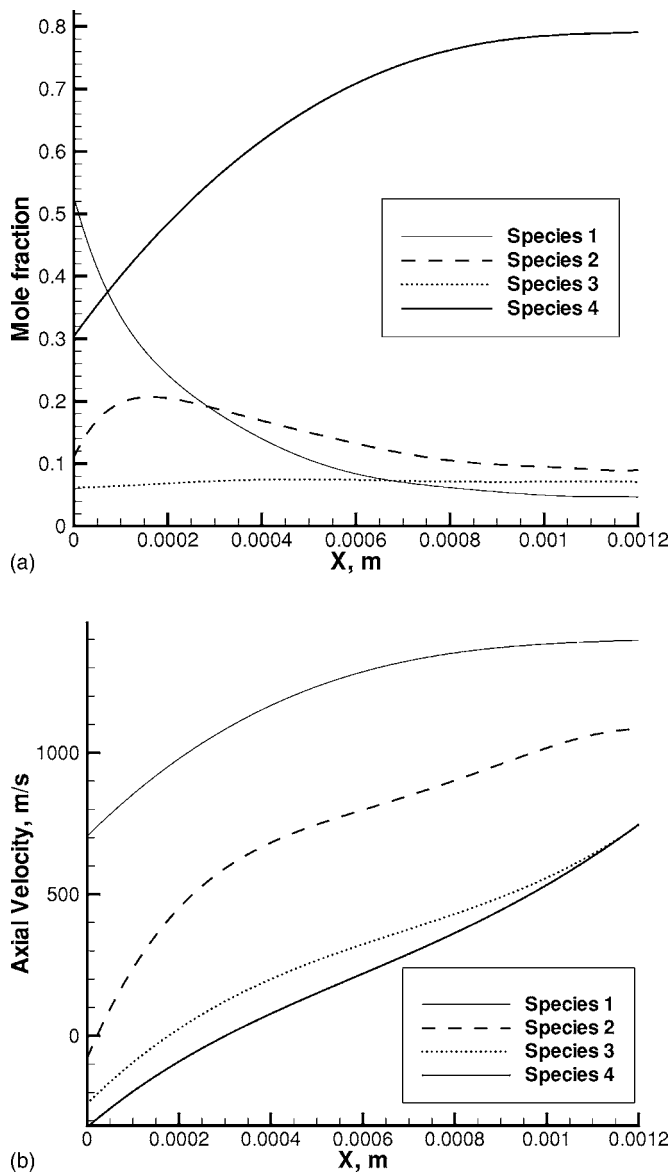


FIG. 12. Distribution of the mole fractions (top) and axial velocities (bottom) of different species along the tube axis. Helium flow, $t/d=1.2$, $P_0=35.7$.

$X=0$ and ends at $X=0.001$ m. Note that although the fraction of molecules with no surface or molecular collisions (species 1) decreases significantly through the tube, it still remains at about 5% at the exit plane. Species 1 is quickly replaced by species 2, 3, and 4. The computation also shows that most particles leaving the tube collide both with the surface and with other particles (species 4).

A small number of particles that do not experience any collisions inside the tube still make significant contribution to the mass flow and momentum flux due to their high axial velocity. As shown in Fig. 12, the average axial velocity of molecules of species 1 at the exit is about two times higher than those of species that collided with the tube surface. The velocity of molecules that have only intermolecular collisions inside the tube is between these two limits. It is obvious that the decrease in the number of intermolecular collisions in gas toward the free molecular regime results in a

larger fraction of molecules of species 1 at the exit plane, and as the result an increase in the mass flow and especially momentum flux. For larger pressures, the average velocity of species 4 is expected to be higher due to the combined effect of molecular collisions on drift velocity.

VIII. CONCLUSIONS

Low density flows through short circular tubes have been studied experimentally and numerically for thickness-to-diameter ratios from 0.015 to 1.2. The nano-Newton Thrust Stand installed in CHAFF-IV was used in the experiments; the computations were performed with the kinetic (the direct simulation Monte Carlo) and continuum (solution of the Navier-Stokes equations) methods. The scope of the work was to examine the mass flow and momentum flux for two gases, helium and nitrogen, in the range of Knudsen numbers from 0.001 to 40. The primary motivation for the work was to study propulsion efficiency of short tubes at low Reynolds numbers, from 0.02 to 770. For the first time, momentum flux through short tubes has been measured, and propulsion efficiency of orifices versus short tubes has been analyzed.

The results obtained with the continuum approach for $\text{Kn} < 0.01$ are in very good agreement with the DSMC predictions in terms of the flow fields, and mass flow, and momentum flux. It was also shown that the numerical predictions of the mass flow/discharge coefficient and momentum flux are in good agreement with the experimental data for all plenum pressures under consideration. The impact of background gas pressure in the chamber was analyzed and found to be insignificant for pressures smaller than 1000 Pa. Although millimeter-scaled configurations have been used in this study, similarity parameters such as the Reynolds and Knudsen numbers allow one to generalize the conclusions of this work to microscale flows. Lately, the area of microscale flows has drawn considerable interest from researchers, which has stimulated the reconsideration of old numerical techniques (such as solutions to the Barnett equations) and the development of new approaches (such as the Information Preservation technique). Excellent agreement between both numerical solutions and the experimental data shows that these more conventional computational approaches are still capable of an accurate prediction of gas flows through short tubes in the entire flow regime from free molecular to continuum. This agreement also indicates that the data, both numerical and experimental, may serve as a reliable basis for comparison and method validation.

The effect of the tube thickness was studied, and a minimum was observed both numerically and experimentally for thick-to-thin orifice ratios of momentum flux versus pressure. The minimum occurs at a Knudsen number between 0.25 and 0.5 and is approximately 10% of the corresponding free molecular values. The minimum in the mass flow ratio on the order of 1% was also shown numerically. The qualitative explanation for the minimum is similar to that of the Knudsen minimum effect; namely, a disproportionately large contribution to mass flow and force from molecules with large axial and small radial velocities. This contribution de-

creases as these molecules collide with molecules reflected from the surface at the flow regime where intermolecular collisions are too rare for a collisional drift to be initiated.

The thick orifice propulsion efficiency is much higher than that of a thin orifice, but does not change significantly when thickness-to-diameter ratio changes from 0.5 to 1. The effect of surface specularity on a thick orifice specific impulse were found to be relatively small.

ACKNOWLEDGMENTS

This work was supported in part by the Propulsion Directorate of the Air Force Research Laboratory at Edwards Air Force Base, California. G.N.M. thanks Jean Muylaert (ESA-ESTEC/TEC-MPA, the Netherlands) for his support of this work, and Paul Pearson (AOES, the Netherlands) for his help with computer resources for the Navier-Stokes computations. S.F.G. and A.D.K. thank Cedrick Ngalande for his assistance with the CHAFF-IV flow analysis.

- ¹A. Jamison, A. Ketsdever, and E. P. Muntz, "Gas dynamic calibration of a nano-Newton thrust stand," *Rev. Sci. Instrum.* **73**, 3629 (2002).
- ²A. D. Ketsdever, M. T. Clabough, S. F. Gimelshein, and A. A. Alexeenko, "Experimental and numerical determination of micropulsion device efficiencies at low Reynolds numbers," *AIAA J.* **43**, 633 (2005).
- ³F. Sharipov and V. Seleznov, "Data on internal rarefied gas flows" *J. Phys. Chem. Ref. Data* **27**, 657 (1998).
- ⁴I. Papautsky, T. Ameel, and A. B. Frazier, "A review of laminar single-phase flow in microchannels," in *Proceedings of the 2001 ASME International Mechanical Engineering Congress*, 11–16 November 2001 (ASME, New York, 2001).
- ⁵M. Knudsen, *Ann. Phys.* **28**, 999 (1909).
- ⁶W. G. Pollard and R. D. Present, "On gaseous self-diffusion in long capillary tubes," *Phys. Rev.* **73**, 762 (1948).
- ⁷A. K. Sreekanth, "Slip flow through long circular tubes," in *6th International Symposium on Rarefied Gas Dynamics* (Academic, New York, 1969), Vol. 1, pp. 667–680.
- ⁸H. Henning, "The approximate calculation of transmission probability for the conductance of tubulation in the molecular flow regime," *Vacuum* **28**, 151 (1977).
- ⁹R. G. Lord, F. C. Hurlbut, and D. R. Willis, "Nearly free molecule flow through a circular orifice at high pressure ratios," in *6th International*

Symposium on Rarefied Gas Dynamics (Academic, New York, 1969), Vol. 2, pp. 1235–1243.

- ¹⁰A. K. Sreekanth, "Transition flow through short circular tubes," *Phys. Fluids* **8**, 1951 (1965).
- ¹¹F. O. Smetana, W. A. Sherrill, and D. A. Schort, "Measurements of the discharge characteristics of sharp-edged and round-edged orifices in the transition regime," in *6th International Symposium on Rarefied Gas Dynamics* (Academic, New York, 1969), Vol. 2, pp. 1243–1257.
- ¹²C. R. Kaplan and E. S. Oran, "Scaling issues for calculations of low-velocity gaseous microflows," in *1999 International Conference on Modeling and Simulation of Microsystems; Nano Science and Technology Institute*, Cambridge, MA, Nano Science and Technology Institute, 1999, pp. 506–509.
- ¹³F. Sharipov and D. Kalempa, "Gaseous mixture flow through a long tube at arbitrary Knudsen numbers," *J. Vac. Sci. Technol. A* **20**, 814 (2002).
- ¹⁴P. Bahukudumbi and A. Beskok, "A phenomenological lubrication model for the entire Knudsen regime," *J. Micromech. Microeng.* **13**, 873 (2003).
- ¹⁵A. Ketsdever, "Thrust measurements of an underexpanded orifice in the transitional regime," in *Proceedings of the 23rd International Symposium on Rarefied Gas Dynamics*, edited by A. Ketsdever and E. P. Muntz (American Institute of Physics, Melville, NY, 2002), pp. 1057–1064.
- ¹⁶A. Alexeenko, S. Gimelshein, D. Levin, A. Ketsdever, and M. Ivanov, "Measurements and simulation of orifice flow for micropulsion testing," *J. Propul. Power* **19**, 588 (2003).
- ¹⁷T. Lilly, N. P. Selden, S. F. Gimelshein, A. D. Ketsdever, and G. N. Markelov, "Numerical and experimental study of low Reynolds number flow through thin-walled orifice and short circular tube," *AIAA Paper No. 2004-2385*, June 2004.
- ¹⁸A. D. Ketsdever, R. H. Lee, and T. C. Lilly, "Performance testing of a microfabricated propulsion system for nanosatellite applications," *J. Micromech. Microeng.* **15**, 2254 (2005).
- ¹⁹N. Selden and A. Ketsdever, "Comparison of force balance calibration techniques for the nano-Newton range," *Rev. Sci. Instrum.* **74**, 5249 (2003).
- ²⁰M. S. Ivanov, G. N. Markelov, and S. F. Gimelshein, "Statistical simulation of reactive rarefied flows: Numerical approach and applications," *AIAA Paper 98-2669*, June 1998.
- ²¹M. S. Ivanov and S. V. Rogasinsky, "Analysis of the numerical techniques of the direct simulation Monte Carlo method in the rarefied gas dynamics," *Int. J. Math. Model.* **3**, 453 (1988).
- ²²G. A. Bird, *Molecular Gas Dynamics and the Direct Simulation of Gas Flows* (Clarendon, Oxford, 1994).
- ²³A. D. Ketsdever, "Facility effects on performance measurements of micropulsion systems that utilize gas expansion," *J. Propul. Power* **18**, 797 (2002).
- ²⁴J. D. Anderson, *Fundamentals of Aerodynamics* (McGraw-Hill, New York, 1984).